

# Infiltrating basal cell carcinoma: a stellate peri-tumor dermatoscopy pattern as a clue to diagnosis

John H. Pyne<sup>1</sup>, Paul Fishburn<sup>1</sup>, Anthony Dicker<sup>1</sup>, Michael David<sup>1</sup>

<sup>1</sup> The University of Queensland, Brisbane, Australia

**Key words:** basal cell carcinoma; dermatoscopy; dermoscopy; infiltrating; skin cancer; vessels

**Citation:** Pyne JH, Fishburn P, Dicker A, David M. Infiltrating basal cell carcinoma: a stellate peri-tumor dermatoscopy pattern as a clue to diagnosis. *Dermatol Pract Concept* 2015;5(2):2. doi: 10.5826/dpc.0502a02

**Received:** May 17, 2014; **Accepted:** January 8, 2015; **Published:** April 30, 2015

**Copyright:** ©2015 Pyne et al. This is an open-access article distributed under the terms of the Creative Commons Attribution License, which permits unrestricted use, distribution, and reproduction in any medium, provided the original author and source are credited.

**Funding:** None.

**Competing interests:** The authors have no conflicts of interest to disclose.

All authors have contributed significantly to this publication.

**Corresponding author:** John H. Pyne, MBBS, BOptom, MMed, PhD, 131 Ellesemere Rd, Gympie Bay, NSW, Australia . Tel. 61.414.750625; Fax. 61.2.95253193. Email: j.pyne@uq.edu.au

**ABSTRACT** **Background:** Infiltrating basal cell carcinoma (BCC) has associated features that may be readily identified using dermatoscopy.

**Objective:** Investigate a stellate dermatoscopy pattern extending from the peripheral margin of infiltrating BCC.

**Methods:** A total of 741 consecutive cases of BCC were assessed retrospectively using non-polarized dermatoscopy. Following histopathologic examination, cases were categorized into six different BCC subtypes. Infiltrating cases numbered 107. This stellate feature was defined as a geometric star shaped pattern extending outwards from the circumferential peripheral edge of the tumor, and identified by white lines, vessels or uneven skin surface morphology. The percentages of infiltrating subtype within the tumor mass and tumor depth were compared, with and without the stellate pattern.

**Results:** Infiltrating BCC displayed the stellate pattern more than other BCC subtypes. Concordance between the two observers was almost perfect for white lines: Kappa coefficient of 0.87 (95% CI: 0.0.79-0.95)  $P < 0.01$  and substantial for vessels: Kappa coefficient of 0.71 95% CI: 0.59-0.84)  $P < 0.01$ . Folds were only recorded in infiltrating cases ( $n=3$ ). Compared to other BCC subtypes the stellate pattern had a sensitivity of 31.7% and specificity of 94.1%. A higher mean fraction of the tumor mass containing infiltrating subtype was found when comparing stellate pattern observed to stellate pattern not observed ( $P < 0.01$ ). No statistically significant association was found between the tumor depth with and without the stellate pattern.

**Conclusion:** This study found a higher incidence of the stellate pattern within infiltrating BCC compared to the other BCC subtypes. As the percentage of the infiltrating subtype within the tumors increased the incidence of the stellate pattern also increased.

## Introduction

Basal cell carcinoma (BCC) is a common primary malignancy of the skin. Different histopathologic subtypes have been recognized and associated with different tumor behaviors. Tumors of the nodular and superficial subtype tend to have indolent behavior compared to those of the infiltrative subtype [1]. Defining key histopathologic features of infiltrating BCC include collagen and fibroblasts in the tumor stroma, basaloid tumor cells in small spiky or angular nests [2] and poorly defined tumor margins. Mixed subtypes are common, particularly infiltrating and nodular subtypes. Examining BCC using dermatoscopy can identify the features associated with these different subtypes. Various pigmented [3-6] and vascular [6,7] dermatoscopy features of BCC have been reported; however, previous studies tend to focus on superficial and/or nodular BCC subtypes. Other BCC histological subtypes display more aggressive clinical behaviors [1], including micronodular, infiltrating and morphoeic BCC, and those BCC with squamous differentiation.

The dermatoscopy features of these more aggressive BCC subtypes have not been extensively studied. When examined using non-polarized dermatoscopy [8], aggressive subtype BCC have been reported to have an absent or lower incidence of pink in the tumor and absent central tumor associated vessels.

Compared with more indolent BCC subtypes, infiltrative BCC have higher rates of incomplete surgical excision [9,10] and perineural invasion [1]. An increased incidence of infiltrating BCC has been reported following involvement, which leads to exenteration of the orbit [11]. Identifying these lesions before surgery can assist planning and management. Anecdotal observation led the authors of this study to investigate a geometrical feature surrounding some BCC observed using dermatoscopy. This feature radiates outwards from the peripheral tumor margin, in a star-like geometrical pattern. The authors propose the term “stellate pattern” to describe this feature.

Blood vessels in a radial distribution have been reported with ulcerated BCC [12]. These vessels are within the dermatoscopy-identified tumor “footprint” or margin. In contrast, the radial blood vessels featured in the stellate pattern extend from the tumor margin out into the surrounding background skin.

Recent studies [13,14] have found differences in dermatoscopy between infiltrating and other BCC subtypes. These differences include a lower frequency of arborizing vessels in infiltrating BCC compared to nodular BCC, reduced frequency of ulceration on infiltrative BCC compared to superficial BCC and a greater frequency of shiny white-red structureless areas within the tumor “footprint” of infiltrating BCC compared to both superficial and nodular BCC [13]. Confocal reflectance microscopy has found compact

collagen surrounding tumor islands to be more frequent in infiltrating (96%) compared to nodular (59%) and superficial (73%) BCC [14].

## Methods

Data collection occurred from 2010 to 2012 in a primary care skin cancer practice in Sydney, Australia. All cases were selected from the routine workflow. All cases were imaged using a non-polarized DermLite FOTO dermatoscope, coupled with a Canon EOS 550D camera. Following imaging, full excision and histopathologic examination, all cases were allocated to various BCC subtypes. Cases were not subjected to a preliminary partial biopsy by punch or shave to determine the histological diagnosis. Cases were excised down to subcutaneous fat as a single surgical procedure, guided by a dermatoscopy tumor margin of at least 1 mm. The authors concede that this did not fully excise all cases due to poor clinical or dermatoscopy margin definition. However, the Authors consider the residual tumor tissue volume in such cases as too small to adversely affect the relevant study results. Data collection was prospective, while dermatoscopy image assessment was retrospective. Each observer was blinded to the BCC subtype diagnosis and to the recordings of the other observer. None of the observers were treating clinicians for any of the study cases.

### Inclusion criteria

All consecutive cases excised within the study timeframe were considered for inclusion. After applying the exclusion criteria, all remaining cases were included in the study.

### Exclusion criteria

Any diagnostic entity other than BCC was excluded. Any collision situation with a BCC and another non-BCC diagnostic entity was excluded. These collisions were based on either clinical, dermatoscopic, or histopathologic assessments. Any known previous surgical or medical intervention involving the BCC or site of excision also led to exclusion. Sites juxtaposed to scars were excluded, as were cases occurring on sites unable to be imaged with dermatoscopy.

### Stellate pattern: definition

The stellate pattern is a geometrical pattern extending from the tumor margin out into the surrounding background skin. This geometrical pattern has a full circumferential distribution and is assessed using clinical examination or dermatoscopy. This pattern has a symmetrical star-like appearance and can be created by blood-filled vessels (see Figure 1), surface morphology folds (see Figure 2), or white linear structures (see Figure 3).

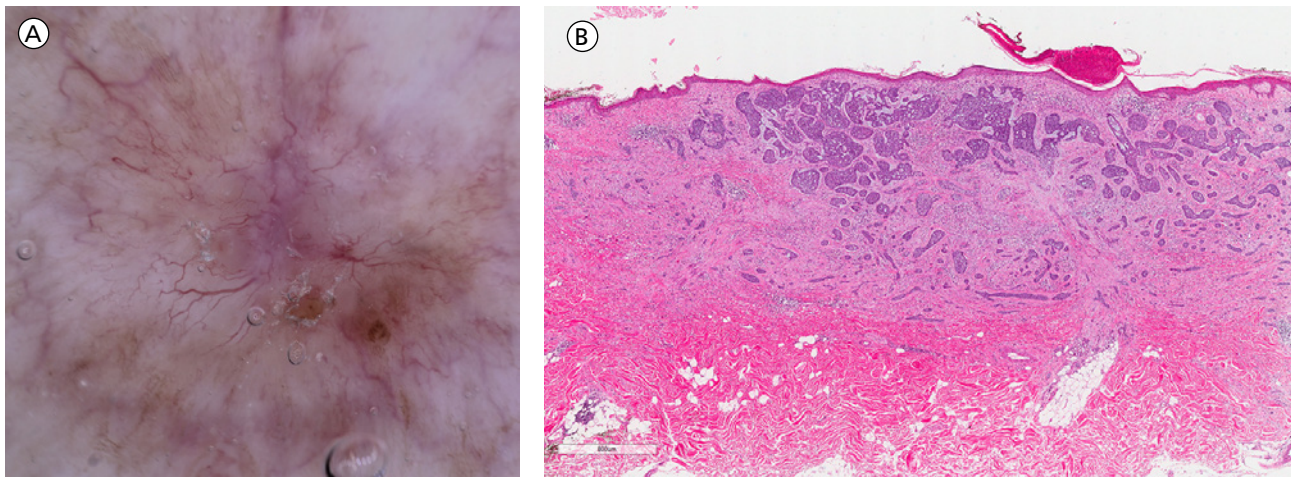


**Figure 1.** (A) Infiltrating basal cell carcinoma on the back, dermatoscopy image: blood-filled vessels displaying a radial stellate pattern. (B) Histopathology of the same lesion, hematoxylin and eosin staining. [Copyright: ©2015 Pyne et al.]

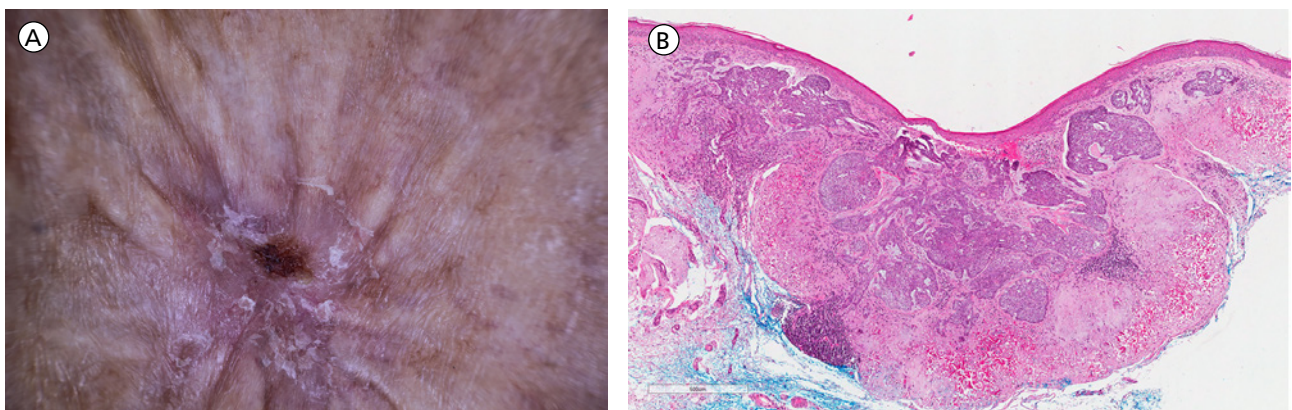


**Figure 2.** (A) Infiltrating and nodular basal cell carcinoma on the neck, dermatoscopy image: folds on the skin surface create a stellate pattern extending from the center of the tumor surface. (B) Histopathology of the same lesion, hematoxylin and eosin staining. [Copyright: ©2015 Pyne et al.]

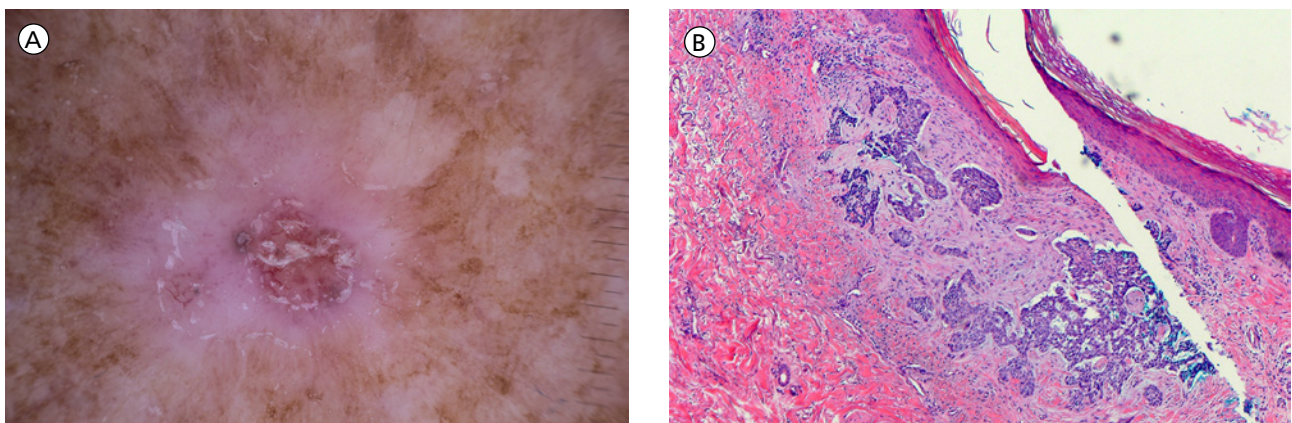


**Figure 3.** (A) Infiltrating and nodular basal cell carcinoma on the leg, dermatoscopy image: circumferential white stellate areas emanating from the peripheral tumor margin. (B) Histopathology of the same lesion, hematoxylin and eosin staining. [Copyright: ©2015 Pyne et al.]

### Stellate pattern: percentage of infiltrating subtype within the tumor

When examining the hematoxylin and eosin stained case slides, a histopathologic assessment of the fraction or percentage of the tumor mass occupied by an infiltrating subtype was estimated to the nearest 10%. A comparison was made between the mean fraction of the infiltrating subtype present for stellate

pattern identified and not identified, for both observers. Due to the presence of non-parametrical distributions, a Mann-Whitney U test #2s sentence 4) or an abridged version of it.eak, irrespective of stellate pattern or observer status, was used to detect the pattern and ob was used to test the equality of group medians. Correlations were equated and assessed by Spearman's rank correlation coefficient, with  $P < 0.05$  con-



**TABLE 1.** Basal cell carcinoma subtypes confirmed by histopathology, frequency of stellate pattern observations. [Copyright: ©2015 Pyne et al.]

BCC subtypes	Total cases n = 741	Stellate pattern identified by both Observers	Stellate white lines identified	Stellate vessels identified	Stellate surface folds identified
Superficial	194 (26.2%)	12 (6.2%)	9 (4.6%)	6 (3.1%)	0
Superficial and Nodular	216 (29.1%)	9 (4%)	9 (4.2%)	3 (1.4%)	0
Nodular	190 (25.6%)	11 (5.8%)	9 (4.7%)	5 (2.6%)	0
Nodulocystic	5 (0.7%)	0	0	0	0
Infiltrating	107 (14.4%)	34 (31.8%)	28 (26.1%)	21 (19.6%)	3 (2.8%)
Aggressive Non- infiltrating	29 (3.9%)	5 (17%)	4 (13.8%)	3 (1.0%)	0

**TABLE 2.** Basal cell carcinoma: variation in the percentage of tumor mass being infiltrating subtype and the presence of a stellate pattern. [Copyright: ©2015 Pyne et al.]

Percentage of tumor occupied by an infiltrating subtype	< 30%	30% to < 70%	70% or more
Number of cases (total = 107)	n = 67	n = 26	n = 14
Stellate pattern identified by both observers	4/67 (6%)	19/26 (73%)	12/14 (86%)

sidered significant. Statistical analyses were conducted using version 12.1 of the STATA software package (StataCorp, College Station, Texas). Ethics approval was obtained from the University of Queensland Ethics Committee.

### Central ulceration on the stellate pattern: a comparison of different basal cell carcinoma subtypes based on central ulceration on the stellate pattern

A cicatricial process from ulceration could be a confounding factor in the presentation of the stellate pattern. To investigate this possible confounding effect a sub-study was performed comparing stellate cases for central ulceration present or absent from the center of the stellate cases for different BCC subtypes.

## Results

Following the application of the inclusion and exclusion criteria, a total of 741 cases remained. These 741 cases were identified on 523 patients who ranged in age from 27 to 98, with a mean age of 61. One of four different pathologists examined each specimen for histological assessment.

The identified subtypes of BCC included superficial, nodular, superficial and nodular combined, nodulocystic, and the collective more aggressive subtypes. The more aggressive group was split into the infiltrative subtype and the other aggressive subtype BCC, see Table 1. The aggressive BCC not of the infiltrative subtype were represented by micronodular and morphoeic BCC, as well as by BCC with squamous differ-

entiation. Infiltrating BCC cases ranged in age from 38 to 96, with 67% being male (n = 72). Table 1 presents the numbers of BCC recorded by histopathologic diagnosed subtype. Table 1 also shows the percentage of lesions identified as having a stellate pattern for both observers and the frequency of each stellate feature. Concordance between the two observers to identify the stellate pattern overall by identifying either white lines, vessels or folds was substantial, with a Kappa value of 0.66 (95% CI: 0.52 to 0.80). Only three cases of folds creating a stellate pattern were recorded, all three cases were infiltrating BCC. The stellate pattern displayed by infiltrating BCC had a sensitivity of 31.7% and a specificity of 94.1%.

As well as identifying the BCC subtypes present, the percentage of the tumor that displayed an infiltrative subtype on the histopathology slides was also assessed. This was graded in increments of 10%. As the percentage of infiltrating subtype increased within the tumor mass, the stellate pattern was recorded with a higher incidence (see Table 2).

An assessment was performed of any association between tumor depth and the percentage of infiltrating subtype present under stellate pattern (observed or not observed). Only one correlation was found to be statistically significant at -0.25 (95% CI: -0.46 to -0.03) for the scenario involving no stellate pattern and observer two (see Table 3).

## Discussion

The data from this study indicate that the stellate pattern has a higher incidence in BCC with the infiltrating or other

**TABLE 3. Correlational analysis between observers. [Copyright: ©2015 Pyne et al.]**

	Observer 1			Observer 2		
	n	r	95% CI	n	r	95% CI
Stellate observed	43	-0.053	-0.348 to 0.251	33	0.084	-0.267 to 0.415
Stellate not observed	64	-0.154	-0.386 to 0.095	74	-0.254	-0.456 to -0.028

r=Spearman's rank correlation coefficient

**TABLE 4. Number of stellate features present within a lesion. [Copyright: ©2015 Pyne et al.]**

BCC subtype	All 3 stellate features present with any lesion	Any 2 features	Only 1 feature	No stellate features present
Superficial n = 42	0	3 (7.1%)	9 (21%)	30 (71%)
Superficial and Nodular n = 39	0	3 (7.7%)	6 (15%)	30 (77%)
Nodular n = 41	0	3 (7.3%)	8 (20%)	30 (73%)
Infiltrating n = 60	2	18 (30%)	10 (17%)	30 (50%)

The three stellate pattern features are either: white lines, vessels or folds. The presence of a stellate pattern was defined as having one or more of any of the three stellate pattern features associated with any lesion. All the above cases were identified by both observers as either stellate present or absent.

more aggressive subtypes, as shown in Table 1. Infiltrating and other more aggressive BCC subtypes typically display histopathology with increased collagen in the tumor stroma. The authors speculate that a contraction effect within the tumor stroma could be one explanation for the development of these stellate patterns. The proportion and location of infiltrating BCC within a BCC of mixed subtypes can vary. One limitation of this study was not assessing the effect of the location of infiltrating BCC within mixed subtype tumors on the incidence of the stellate pattern. Another limitation of this study was using non-polarized dermatoscopy alone. Using polarized dermatoscopy may produce different vessel and white structures results.

Tumors with a stellate pattern were found to contain a higher mean fraction of infiltrating BCC within the tumor mass compared to cases not displaying a stellate pattern. This mean fraction finding was significant and consistent for both observers. The relationship between tumor depth and percentage of infiltrating subtype present was found to be weak at best, irrespective of stellate pattern or observer status. We hypothesize the stellate pattern is dependent on sufficient infiltrating tumor occupying the papillary dermis. Future investigation comparing infiltrating BCC involving predominantly the papillary dermis to infiltrating tumor predominately within the reticular dermis may produce different stellate pattern results rather than comparing depth alone.

This study identified that these stellate patterns around a BCC provide an *in vivo* clue to the increased possibility of

the presence of an infiltrating BCC subtype. Combinations of the stellate features (white lines, vessels or folds) significantly increase the chance of a BCC being an infiltrating BCC. A Chi-square test showed that BCC subtype and number of stellate pattern features was significantly related ( $p < 0.01$ ), with infiltrating BCC more likely in those with multiple stellate features, see Table 4.

To assess the potential for the stellate pattern to be confounded by ulcer induced cicatrization within infiltrating BCC we compared the presence or absence of central ulceration on stellate cases between different subtypes of BCC. Table 5 sets out the recorded presence of central ulceration by BCC subtype. Nodular BCC with a stellate pattern (n=11) had central ulceration on 5 cases (45%). Stellate cases of infiltrating BCC (n=34) displayed central ulceration in 17 cases (50%). These very similar findings for the two different subtypes of BCC suggest that central ulceration is both not essential for the stellate pattern and not unique to infiltrating BCC. The typical histopathology of nodular BCC does not include cicatrization. Future work could examine if there is any spatial correlation between prominent central ulceration on the stellate pattern and any associated histopathologic cicatrization.

Future investigation may assess the incidence and character of stellate patterns in diagnostic entities, as well as BCC. The stellate sign was not pathognomonic for the diagnosis of infiltrative BCC. However, identifying this dermatoscopy feature may help guide clinicians in their approach to managing the tumor.

**TABLE 5. Basal cell carcinoma with the stellate pattern identified by both observers: incidence of ulceration located at the centre of the stellate pattern. [Copyright: ©2015 Pyne et al.]**

Basal cell carcinoma subtype with stellate pattern present	Ulceration at the centre of the stellate pattern
Superficial n = 12	3 (25%)
Superficial and Nodular n = 9	1 (11%)
Nodular n = 11	5 (45%)
Infiltrating n = 34	17 (50%)

## Conclusion

BCC may display a stellate pattern extending from the periphery of the tumor when examined using dermatoscopy. These stellate patterns may be represented by white lines, blood vessels or surface folds in a circumferential radial pattern extending outwards beyond the tumor margin. When present, these stellate patterns may offer a clue to the presence of an infiltrating BCC subtype.

## References

1. Crowson AN. Basal cell carcinoma: clinical features, histology, and biology. In: Crowson AN, Magro C, Mihm MC Jr. *Biopsy Interpretation of the Skin: Primary Non-Lymphoid Cutaneous Neoplasia*. Philadelphia, PA: Lippincott Williams Wilkins, 2010:199-234.
2. Sexton M, Jones DB, Maloney ME. Histologic pattern analysis of basal cell carcinoma. *J Am Acad Dermatol* 1990;23(6):1118-26.
3. Menzies SW, Westerhoff K, Rabinovitz H, et al. Surface microscopy of pigmented basal cell carcinoma. *Arch Dermatol* 2000;136(8):1012-16.
4. Demirtasoglu M, Ilknur T, Lebe B, et al. Evaluation of dermoscopic and histopathologic features and their correlations in pigmented basal cell carcinomas. *J Eur Acad Dermatol Venereol* 2006;20(8):916-20.
5. Scalvenzi M, Lembo S, Francia MG, et al. Dermoscopic patterns of superficial basal cell carcinoma. *Int J Dermatol* 2008;47(10):1015-18.
6. Altamura D, Menzies SW, Argenziano G, et al. Dermatoscopy of basal cell carcinoma: morphologic variability of global and local features and accuracy of diagnosis. *J Am Acad Dermatol* 2010;62(1):67-75.
7. Micantonio T, Gulia A, Altobelli E, et al. Vascular patterns in basal cell carcinoma. *J Eur Acad Dermatol Venereol* 2011;25:358-61.
8. Pyne J, Sapkota D, Wong JC. Aggressive basal cell carcinoma: dermoscopy vascular features as clues to the diagnosis. *Dermatol Pract Conc* 2012;2(3):2.
9. Su SY, Giorlando F, Ek EW, et al. Incomplete excision of basal cell carcinoma: a prospective trial. *Plast Reconstr Surg* 2007;120(5):1240-8.
10. Farhi D, Dupin N, Palangie A, et al. Incomplete excision of basal cell carcinoma: rate and associated factors among 362 consecutive cases. *Dermatol Surg* 2007;33(10):1207-14.
11. Iuliano A, Strianese D, Uccello G, et al. Risk factors for orbital exenteration in periocular basal cell carcinoma. *Am J Ophthalmol* 2012;153(2):238-41.
12. Rosendahl C, Cameron A, Tschandl P, et al. Prediction without pigment: a decision algorithm for non-pigmented skin malignancy. *Dermatol Pract Concept*. 2014;4(1):9.
13. Lallas A, Tzello T, Kyrgidis A, et al. Accuracy of dermoscopic criteria for discriminating superficial from other subtypes of basal cell carcinoma. *J Am Acad Dermatol* 2013;70(2):303-11.
14. Longo C, Lallas A, Kyrgidis A, et al. Classifying distinct basal cell carcinoma subtype by means of dermatoscopy and reflectance confocal microscopy. *J Am Acad Dermatol* 2014;71(4):716-24.